Acta Mechanica Solida Sinica, Vol. 29, No. 3, June, 2016 ISSN 0894-9166
Published by AMSS Press, Wuhan, China

Helical Fiber Pull-out in Biological Materials**

Lixin Wang[1] **Yuhong Cui**[1] **Qinghua Qin**[2] **Hui Wang**[3] **Jianshan Wang**[1]*

([1] *Tianjin Key Laboratory of Modern Engineering Mechanics & Department of Mechanics, Tianjin University, Tianjin* 300072*, China*)

([2] *Research School of Engineering, Australian National University, Canberra, ACT*0200*, Australia*)

([3] *Department of Engineering Mechanics, Henan University of Technology, Zhengzhou* 450001*, China*)

Received 30 September 2015, revision received 5 May 2016

ABSTRACT Many biological materials, such as wood and bone, possess helicoid microstructures at microscale, which can serve as reinforcing elements to transfer stress between crack surfaces and improve the fracture toughness of their composites. Failure processes, such as fiber/matrix interface debonding and sliding associated with pull-out of helical fibers, are responsible mainly for the high energy dissipation needed for the fracture toughness enhancement. Here we present systemic analyses of the pull-out behavior of a helical fiber from an elastic matrix via the finite element method (FEM) simulation, with implications regarding the underlying toughening mechanism of helicoid microstructures. We find that, through their uniform curvature and torsion, helical fibers can provide high pull-out force and large interface areas, resulting in high energy dissipation that accounts, to a large extent, for the high toughness of biological materials. The helicity of fiber shape in terms of the helical angle has significant effects on the force-displacement relationships as well as the corresponding energy dissipation during fiber pull-out.

KEY WORDS biological materials, helicoid microstructures, fiber pull-out, energy dissipation, toughness

I. Introduction

Through over a billion years' evolution, many high-performance and extremely efficient biological materials have been produced naturally in plants and animals, for example, bone, nacre, wood, and climbing tendrils, resulting from stringent selection processes[1–8]. By combining the optimized hierarchical organizations and hybridization among multiple chemical components, these biological materials can induce some remarkable properties including high strain hardening and high toughness and strength to adapt to various environmental conditions and fulfill their biological functions[9]. The mechanisms and principles behind the outstanding properties and functions of these biological materials can provide a source of inspiration to guide the design and fabrication of novel materials. Understanding and unravelling the underlying composition-structure-property-function relationships of biological materials have been promising and challenging issues fascinating researchers in the fields of physics, materials science, and engineering in recent decades.

Most biological materials have hierarchical structures covering the levels from atomic scale to nano- and microscale in terms of characteristic dimensions. Through their synergistic interactions, these

* Corresponding author. E-mail: wangjs@tju.edu.cn

** Project supported by the National Basic Research Program of China (No. 2012CB937500) and the National Natural Science Foundation of China (Nos. 11272230, 11472191 and 11172207).

microstructures can perfectly dedicate themselves at different levels, resulting in superior integrated properties. For example, the recognized brick-and-mortar-like microstructure with nanosized thin mineral platelets embedded in protein matrix provides nacres, bones, and teeth with superior toughness and strength, whereas the great diversity of micro- and nanostructures of plants (e.g., lotus and lily) leaf surfaces and animal legs provides these structures with their multifunctional properties such as hydrophobicity[3,4,6,10,11]. The formation of microstructures, for example, the biomineralization process or the assembly of biopolymers, is usually a structural evolution and optimization of chemical, physical and biological components at a number of length and time scales. Generally, the elaborated microstructures in biological materials are assembled from weak constituents following clearly defined patterns or shapes[8,9]. For example, the nanosized mineral platelets in bone and nacre, usually with a large aspect ratio, are made of stiff/brittle inorganic constituents, whereas fibers (or cells) in wood are made of cellulose, hemicellulose, and lignin[1,3,4,12,13]. The size, shape, arrangement and components of microstructures play crucial roles in the realization of the outstanding mechanical and physical properties and functions of biological materials.

The common building blocks of biological materials or tissues, such as DNA, proteins, and celluloses, usually have intrinsic chirality in their geometric configurations[14]. That means there is an absence of mirror symmetry of biomacromolecules in these materials, a feature that particularly favors chiral assembly or growth, forming a variety of chiral microstructures, e.g., helical inclusions and twisted arrangements of constitute elements, at multiple length scales[15]. Moreover, some other factors associated with growth or assembly, such as inhomogeneous interactions between organic and inorganic components and anisotropic physical or chemical environments, can also induce helical or twisted microstructures. Among the intricate microstructures developed in nature, chiral microstructures are perhaps most pervasive[14] and have attracted significant attention from researchers. Chiral microstructures appear at almost every structural level of biological materials[7,14]. For example, chiral structured motifs exist at nano- and microscale, and even in a hierarchical manner, in DNA, wood, tendon, ligament, bone, hoof, and horn, to name just a few. In fact, biological microstructures taking chiral shapes such as the helix can even be regarded as a unifying structural principle in biology[14]. Several representative chiral microstructures in animal and plant tissues are shown in Fig.1. Figure 1(a) shows that nanoscale cellulose fibril helices, as the building block of tendrils of a towel gourd[7], are contained in the cell wall. Figure 1(b) shows that a chiral stack microstructure is composed of densely packed helical fibrils in the shell of the pteropod *Clio pyramidata*[16]. Similar helical or twisted arrangements of mineral rods also occur in the crab exoskeleton, forming the Bouligand structure, as shown in Fig.1(c)[1]. In Fig.1(d) it can be seen that the cell wall in wood consists of several cylindrical helicoid layers, each layer being made up of a number of cellulose fibrils helically winding in a matrix of hemicellulose and lignin with different microfibril angles (MFAs)[8,12]. As a unique structural motif, such three-dimensional microscopic helicoid layers are also present in many other biological materials such as bone. Figure 1(e) demonstrates that, like the wood cell wall, the osteon, as the building block of bone, is composed of the haversian canal and multiple mineral lamellae, in which collagen fiber is helically intercalated with a definite MFA[1]. At nanoscale, the collagen fiber is a bundle of collagen fibrils in a form of a triple helix structure, demonstrating a hierarchy of chiral microstructure. In fact, a number of animal and plant tissues such as tendons, ligaments, and climbing tendrils are hierarchically structured chiral materials.

Extensive helical or twisted microstructures can not only expertly control the macroscopic morphologies of plant tissues such as climbing tendrils through varying the size and shape of the microstructures[7], but also provide biological materials with a wide range of superior physical and mechanical properties. For example, the helical winding of cellulose or collagen fibrils in the basic building elements endows wood and bone with unusual piezoelectricity; helical nanostructures render the beautiful and brilliant colors of butterfly wings[17]. This is because, due to their inherent geometrical chirality, i.e., translation-rotation helical symmetry, helical or twisted microstructures usually bring a corresponding chirality to certain material properties, a feature normally manifested by the electro-mechanical coupling behavior and the stretch-twist coupling deformation, etc.[18,19]. Compared to their straight or planar counterparts, chiral microstructures are more extensible and flexible due to their three-dimensional configurations with uniform curvature and torsion[20]. Furthermore, chiral microstructures often induce a hardening type nonlinear constitutive behavior, providing their composites with a relatively high ability of energy absorption during deformation and rupture[20]. For example, coarse-grained simulation results show

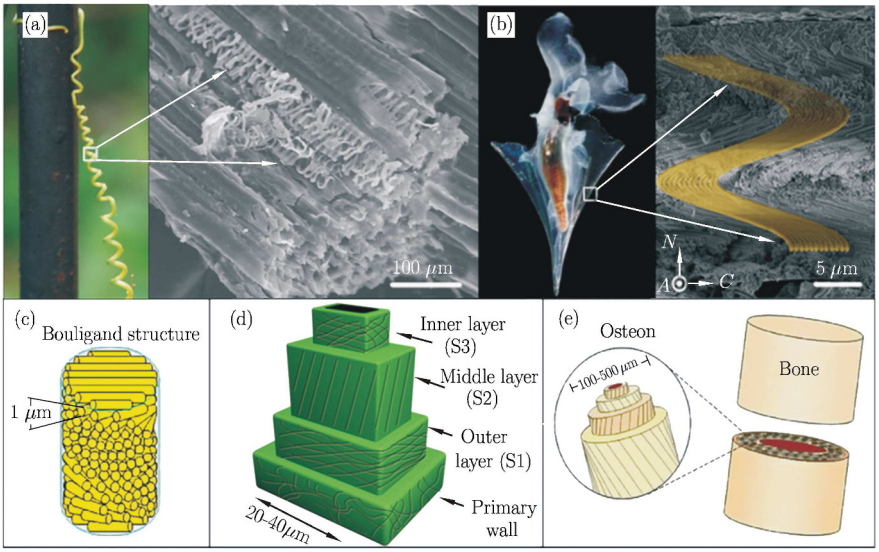

Fig. 1. Helical microstructures in biological materials. (a) Towel gourd tendril and its microscopic structures (Figure reproduced from Ref.[7]); (b) Shell of the pteropod *Clio pyramidata* and its cross-sectional-view SEM images of fracture surface (Figure reproduced from Ref.[16]); (c) Schematic diagram of Bouligand structures in crab exoskeleton (Figure reproduce from Ref.[1]); (d) Schematic diagram of helicoid microstructures in wood cell wall; (e) Schematic diagram of helicoid microstructures in osteon of bone (Figure reproduced from Ref.[1]).

that under axial stretch, the wood cell wall undergoes elastic, slip-stick plastic, and high strain stiffening deformation, all of which are controlled by the helical winding angle of cellulose fibrils[13]. Thus, in natural and human-made materials, chiral microstructures usually serve as reinforcing structural elements to achieve high toughness. Dynamic fracture experiment results of helical-fiber/metal-matrix composite have shown that initial twisting of the fiber can effectively improve the toughness of a composite[21]. Recent study has demonstrated that, through tortuous crack propagation, a helical microstructure consisting of interlocking nanofibers can effectively constrain mechanical damage to the shell of the pteropod *Clio pyramidata* and thus distinctly improve the fracture toughness of the shell[16]. Wood and bone, two typical load-bearing materials in nature, achieve their high toughness through synergistic interactions of microstructures at different length scales. As the basic building block elements of wood and bone, helicoid microstructures play crucial mechanical roles in the high ability of wood and bone to resist fracture. In bone, the helical packing of the collagen fibrils in minor lamellae enhances the elastic modulus, the work of fracture, and the breaking strain of hydroxyapatite[22]. Notably, the high fracture toughness of wood is greater than that predicted for a simple fibrous composite by about 20%. Such a great difference in the value of the fracture toughness of wood is attributed, to a large extent, to the helical winding of cellulose fibers in the multilayered cell walls[22].

Previous studies of traditional fiber composites have shown that fracture toughness enhancement is contributed mainly from the high energy dissipation during failure processes such as the fiber/matrix interface debonding and sliding associated with fiber pull-out. For that reason, the pull-out of fiber from matrix has attracted a great deal of research during past decades. The pull-out behaviors of straight fibers and fibers with planar shapes, such as curved fibers from an elastic matrix in composites, have been extensively investigated using theoretical models and computational simulations. For example, Fu et al. theoretically investigated the pull-out of fibers with branched structures from a matrix and found that such branched structures of fibers could effectively enhance the strength and fracture toughness of their composites[23]. Fu and Lauke studied the effects of fiber length and distributions of fiber orientation on the fiber pull-out energy of short fiber composites[24]. Xu et al. proposed a micromechanical damage-plasticity formulation to analyze the dissipated energy of pull-out of a steel fiber with a single hooked end from a cement-based matrix[25]. Chen et al. analytically investigated the bonding, interfacial debonding and sliding of curved-fiber pull-out in nanotube-reinforced polymer composites[26]. Chen et al. conducted a multi-scale failure analysis of carbon nanotube-reinforced composites, including CNT pull-out and

breakage[27]. Yang et al. investigated the size effects of fiber pull-out[28]. Shi et al. studied the effects of helically shaped nanotubes on the elastic properties of carbon nanotube-reinforced composites[29]. However, the failure process of helicoid microstructures, such as the pull-out of helical or twisted fiber, has not yet been studied, although chiral microstructures exist widely in biological materials and play an important role in achieving high toughness. Compared to straight and planar shaped fibers, helical fiber shapes usually induce much more complex three-dimensional stress and strain fields, and thus at present there are generally no analytical solutions for helical fiber pull-out.

In wood and bone, helicoid microstructures are made up of relatively weak components such as cellulose and lignin or hydroxyapatite and protein molecules, yet they exhibit high toughness. Their structural features and mechanical mechanisms therefore have the potential to inspire the development of novel materials with enhanced properties. Investigation of such underlying mechanisms or principles should foster new understandings of how biological materials assemble weak components at nano- and microscale to achieve such high mechanical properties. From a biomimetic point of view, it is critical to identify the exact underlying mechanisms at nano- and microscale that control the high toughness of biological materials.

In this paper, we quantitatively investigate the pull-out behavior of a helical fiber from an elastic matrix using the FEM simulation, with implications for the mechanism underlying the mechanical reinforcement of helicoid microstructures.

II. FEM Modeling of Helical Fiber Pull-out

In bone and wood, helicoid microstructures such as osteon and wood cell or fiber usually have a large aspect ratio. For example, the length of an osteon or plant cell is of the order of several millimeters, whereas their width is only about several micrometers and even tens of nanometers. Both bone and wood derive their mechanical properties mainly from the basic structural elements, i.e., osteon and plant cell. In this sense, we can simply consider bone and wood as fiber-reinforced composites, although they have complex hierarchical structures. Compared to traditional fiber-reinforced composites, crack propagation in wood and bone and the corresponding failure processes are much more complex, usually involving deformation and fracture of microstructures at multiple length scales and their interplay. The failure process typically involves deformation and cracking of hierarchical microstructures, debonding of interface between fiber (i.e., osteon and plant cell) and matrix, fiber pull-out and even breakage. It is noted that fiber pull-out and breakage can occur simultaneously in some cases, depending on the interface strength, fiber strength, and fiber modulus[30]. Compared to straight fibers, helical fibers can usually tolerate large elongation while still retaining low strain, due to their geometrical shapes. In this paper, we mainly elaborate on the effects of the helical shape of microstructure on pull-out behaviors, and thus the fiber breakage is not considered. The failure process also includes debonding and frictional sliding of the interface between the helicoid layers in osteon and wood cell wall. Among these important failure mechanisms, fiber/matrix interface debonding and fiber pull-out are considered as the most significant sources of energy dissipation that accounts for the high toughness of bone and wood. As shown in Fig.2, wood cells are often pulled out from their matrix during the fracture process of wood, serving as bridging elements to transfer stresses between crack faces. The geometrical shape and size of bridge elements and their arrangements are, to a large extent, responsible for the tensile and shear stresses and the corresponding energy dissipation in the bridging zone. Therefore, particular attention is warranted on the way helicoid microstructures contribute to the high toughness of their composites.

In this study we take wood as an example, and conduct the FEM simulation of pull-out behaviors of helical fibers, with implications for the underlying mechanism whereby helicoid microstructures enhance the fracture toughness of biological composites. In our simulation and analysis, we use for simplicity a model of a composite system for wood. Among the helicoid layers in the wood cell wall, the secondary layer (i.e., S2 layer) with the greatest thickness is generally considered to be directly responsible for the mechanical properties of the cell. Thus, only the S2 layer is considered and other helicoid layers can be neglected, again for simplicity. Taking wood as a fiber composite[31], the traditional single-fiber concentric cylinder system in which a straight fiber or cell wall is embedded in a cylinder matrix can be used as the composite system model in our analysis to represent the wood cell and surrounding matrix material. Considering the fact that the primary structured characteristic of the S2 layer in the fiber or wood cell wall lies in the helical winding of cellulose microfibrils, the composite system model can be further

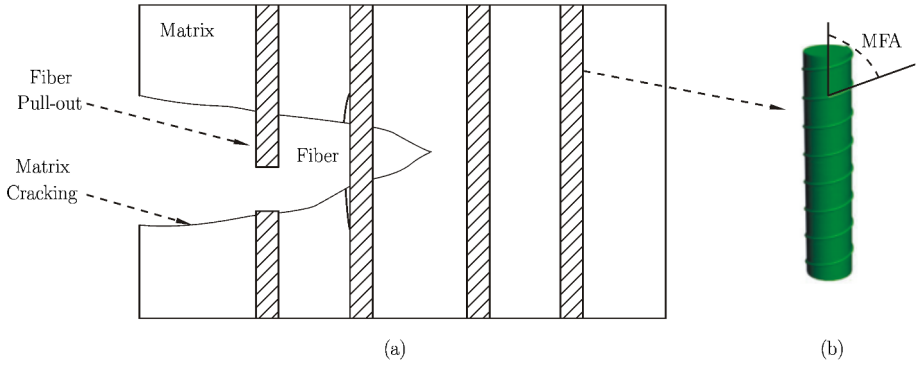

Fig. 2. (a) Schematic diagram of bridging fiber in composite; (b) Fiber with helical winding of cellulose microfibril.

simplified as a right-handed helical-fiber concentric cylinder as shown in Fig.3(a), in which a helical fiber is embedded in the cylinder matrix. The present study focuses mainly on the load-displacement relationships and the corresponding energy dissipation during the pull-out process of the helical fiber. ABAQUS software[32] is used for the FEM simulation. In our simulation, the cross-sectional radius of the fiber and cylinder matrix is $r_f = 40\,\text{nm}$ and $R_m = 0.75\,\mu\text{m}$, respectively. The thickness of the matrix is taken as $H = 1.5\,\mu\text{m}$. The helical fiber with a uniform helical radius $R_h (R_m >> R_h >> r_f)$ is located in the elastic matrix along the central line. The fiber and matrix are considered to be linearly elastic and isotropic. The matrix is considered a wood material. It is demonstrated that elastic modulus of the wood usually ranges from 0.5 GPa to 20.0 GPa and the Poisson's ratio is about 0.3∼0.5, depending on the values of the MFAs and the positions on the annual rings of cross-section[33–35]. Thus, the property parameters of matrix are taken reasonably as $E_m = 0.8\,\text{GPa}$ for elastic modulus and $\nu_m = 0.33$ for Poisson's ratio. The fiber is assumed to be made of cellulose microfibrils. The elastic modulus and Poisson's ratio of the fiber are $E_f = 2.5\,\text{GPa}$ and $\nu_f = 0.4$, respectively. The finite element mesh used in the simulation is shown in Fig.3(b). The C3D8R elements and C3D10M elements[32] are adopted for the helical fiber and matrix, respectively. The cohesive interface element COH3D8[32] with zero thickness is used to simulate the fiber/matrix interface. It is assumed that the interface exhibits a bilinear constitutive relationship, i.e., the cohesive law, between the tractions T acting on the interface and the corresponding interfacial separation Δ (the displacement jump across the interface). The maximum nominal stress criterion is utilized to describe failure of the cohesive interface, in which the damage or debonding of the interface is assumed to initiate when the nominal stress components of the cohesive interface reach their maximum[32]. The friction sliding is assumed to obey the Coulomb's law of friction, with

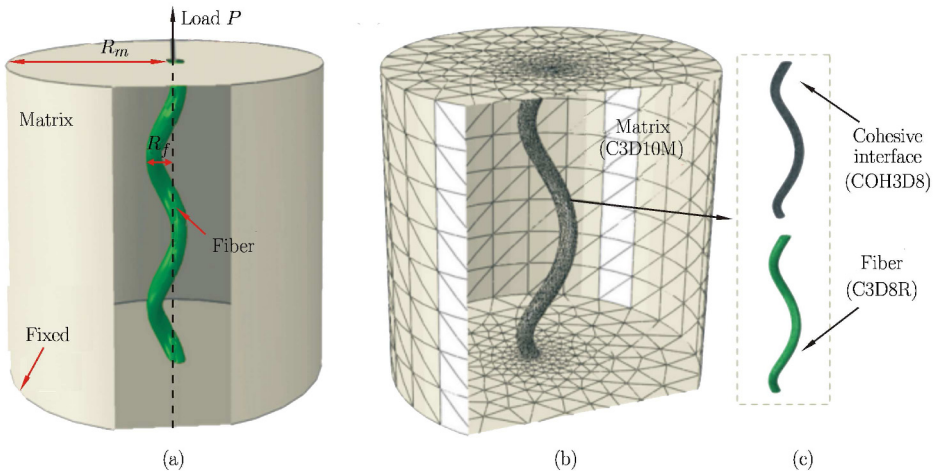

Fig. 3. (a) Schematic diagram of helical-fiber/matrix system subjected to a tension loading; (b) FE meshing of fiber and matrix; (c) Type of finite elements utilized in fiber and the fiber-matrix interface.

a constant friction coefficient. The boundary conditions imposed on the model are similar to those of a typical single-fiber pull-out test. On the top of the helical-fiber concentric cylinder, a tensile loading P along the centerline of cylinder is applied on the fiber end and the surface of matrix end is kept free of stress. At the bottom of the cylinder, the displacements of the matrix end are constrained and the fiber end is kept free. The fiber/matrix interface at the initial state is assumed to be perfectly bonded, and is assumed to be able to slide after the onset of interface debonding. The displacement components of fiber and matrix maintain the continuity at the bonding interface. Element sizes are selected by continuously refining the mesh until approximate convergence of the numerical solution is obtained.

III. Results and Discussion

In this section we focus mainly on the energy dissipation mechanism from the force-displacement response curves in a single helical fiber pull-out process, and also illustrate the complicated interfacial zone evolution during helical fiber pull-out. In contrast to a straight fiber, each section of the helical fiber is differentially subjected to twisting, bending, and axial extension deformations due to the uniform curvature and torsion, leading to a complex stress field[20]. Under the action of pull-out force P, mainly axial stress, hoop stress, and shear stress exist in the fiber. In contrast to the straight fiber, the shear stress components direct along the circumference of the fiber cross-section and the helical center line due to the twisting deformation of the fiber, which contributes together to the debonding or failure of the interface. In Fig.4, the pull-out force-displacement curves are plotted for different MFAs to show the effect of helicity of the fiber. Considering the fact that, in biological materials, the end of the fiber is often fully bonded with the matrix during the fracture process, the twisting freedom of the fiber end at which the pull-out force has been applied is constrained. It is seen from Fig.4 that a typical force-displacement curve of the pull-out of the helical fiber includes three regions that are similar to those found in the pull-out of straight fiber. At the initial stage, a linear response to the increasing force corresponds to the perfect fiber/matrix bonding. Then, as the pull-out force increases, fiber/matrix interface debonding or crack occurs, beginning to propagate stably along the helical interface, and resulting in a generally nonlinear force-displacement relationship. When the crack length reaches a critical value, the crack propagation becomes unstable and usually leads to sudden interface debonding. Finally, frictional sliding of the fiber begins until it is pulled out. Figure 4 shows that the pull-out force is distinctly increased by the relatively high MFA during the fiber debonding and frictional sliding stages. The MFA denotes the degree of helicity of the fiber shape. For example, MFA = 0 signifies that the fiber is straight in the axial direction. Such results suggest that the helicity of fiber shape can effectively enhance the values of the pull-out force at which fully debonding and frictional sliding of interface occur. Correspondingly, variations of the dissipation of energy with displacement are given in Fig.5. Dissipation energy refers to the energy dissipated during the pull-out process. During helical fiber pull-out, only debonding of the fiber/matrix interface and the subsequent frictional sliding between fiber and matrix dissipate energy, with the latter accounting for a large proportion. In the initial stage, only linear deformation occurs and almost no dissipation of energy occurs. As shown in Fig.5, energy dissipations increase to a high value after undergoing a nonlinear increase during the interface debonding

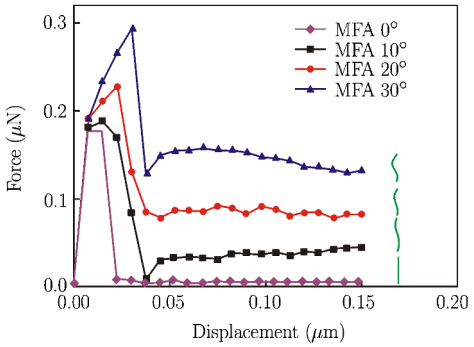

Fig. 4. Pullout force-displacement curves for different MFA when twisting of the loading end is constrained.

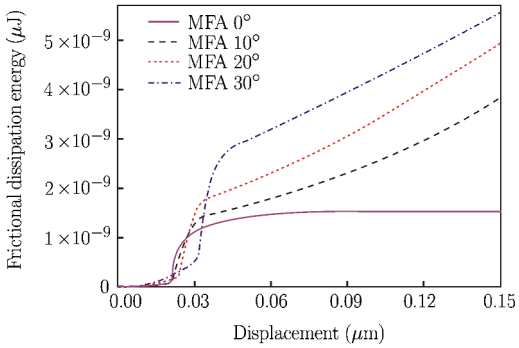

Fig. 5. Energy dissipation during pull-out of helical fiber corresponding to Fig.4.

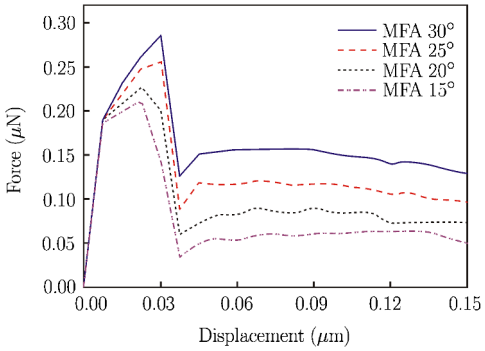

Fig. 6. Pull-out force-displacement curves for different MFAs and the same fiber length.

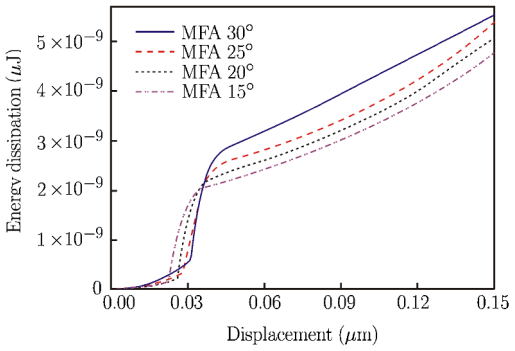

Fig. 7. Energy dissipation during pull-out of helical fiber corresponding to Fig.6.

stage and a linear increase during the frictional sliding stage. This is because frictional sliding obeys the Coulomb friction law and thus the corresponding linear energy dissipation depends on the sliding length. Obviously, compared to the straight shape, a helical shape with large MFA usually results in much higher values of pull-out force and energy dissipation. It should be noted that the fibers considered in Figs.4 and 5 corresponding to the plotted curves that have different MFAs and fiber lengths and the same helical radius, implying that these composite systems have different fiber volume percentages (FVPs). To further illustrate the effects of MFA, we also plot the force-displacement curves shown in Fig.6 and the variation curves of energy dissipation shown in Fig.7 in the case that the considered composite systems have the same FVP, that is, only the MFA varies and the fiber length is unchanged. The FVP of the composite system with a straight fiber can be defined as $V_f^s = r_f^2/R_m^2$ and with a helical fiber as $V_f^h = \dfrac{\pi r_f^2 L}{\pi R_m^2 L \sin\alpha} = r_f^2/(R_m^2 \sin\alpha)$, in which the helical angle $\alpha = 90° - \text{MFA}$ and L denotes the fiber length. This definition shows that the FVP of the helical fiber depends on the fiber cross-section radius, the matrix cross-section radius, and the helical angle. When the FVP is fixed, the values of fiber radius can be determined if the value of MFA is given. For a helix, the fiber length can be expressed as $L = 2n\pi R_h/\cos\alpha$, in which n denotes the coil number and the helical angle $\alpha = 90° - \text{MFA}$. The geometrical configuration (e.g. helical radius) of fiber helices with a fixed length and one coil can also be determined for a definite value of MFA. The fiber length is taken as $L = 1.73\,\mu$m. Figures 6 and 7 show that a higher MFA can result in higher values of both pull-out force and energy dissipation, which are similar to those in Figs.4 and 5. These results in Figs.4-7 indicate that the MFA of the fiber can effectively control the values of pull-out force energy dissipation. It should be noted that in wood, MFA values generally range from zero to 45°. On the one hand, the uniform curvature and torsion of the helical center line of the fiber induce a combination of the axial shear stress along the center line and the circumferential shear stress of the fiber cross-section, which generates a much higher pull-out force than that of the straight fiber. On the other hand, helices have been proved to be the optimal shape adopted by long thin strings such as DNA and folded polymeric chains to achieve the greatest length or the highest compact density in a limited space[36]. Similarly, the helical shape also leads to the greatest length of fiber as well as the largest interface area for the helical-fiber/matrix system with a specified thickness. Thus, the combination of these two sides induced by the helical shape of the fiber results in energy dissipation during fiber pull-out that is much higher, even several times greater than that in a straight-fiber/matrix cylinder system. In fiber composites, the energy dissipation of fiber pull-out is the main contributor to the toughness of the composite. Therefore, the helical shape of a fiber at microscale can be considered as one of the main sources of the high toughness of wood and bone. That toughening mechanism of helical fibers at microscale can effectively explain the aforementioned great difference between the real value of the fracture toughness of wood and its predicted value using a simple fibrous composite model.

Figure 8 illustrates the effects of fiber length on the force-displacement relationship of the fiber pull-out. During the computation, the MFA is fixed at 30°. The parameters of fiber and matrix properties are taken as those from Fig.4. It is shown that at the fully bonded stage, the fiber length has no distinct

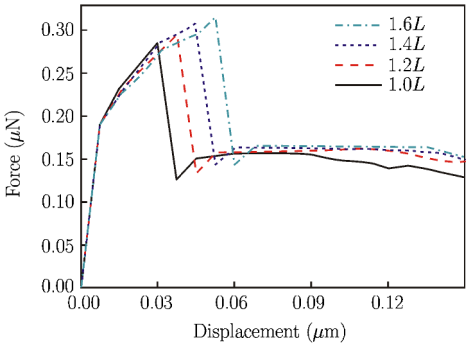

Fig. 8. Pull-out force-displacement curves for different fiber lengths and different MFAs.

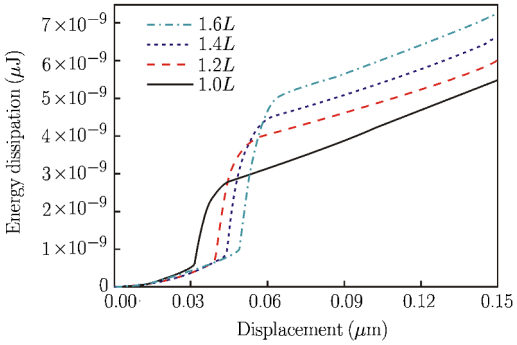

Fig. 9. Energy dissipation during pull-out of helical fiber corresponding to Fig.8.

effect on the pull-out behavior. However, the fiber/matrix interface debonding force and the friction force clearly increase with the increase of fiber length. Correspondingly, the energy dissipation during these two stages can also be affected by fiber length, as shown in Fig.9. This phenomenon suggests that an increase in fiber length can directly increase the interface area, and in turn, increases both the debonding force and the dissipated energy. Moreover, the size of the fiber cross-section can also distinctly influence fiber pull-out behaviors. In Fig.10, the force-displacement curves for different fiber radii are plotted. We take MFA $= 30°$ and $r_f = 40\,\text{nm}$. It can be found that the force during the pull-out process can be effectively increased by increasing the cross-section size. Because the FVPs of the composite systems under consideration are directly proportional to the MFA and fiber cross-section radius for the same fiber length, the results in Fig.10 in fact show that the effects of FVP on the pull-out behavior are similar to those of fiber cross-section.

Figure 11 shows the force-displacement curves for different MFAs, in which the loading end of fiber can twist freely during fiber pull-out. Except for the boundary condition of the fiber loading end, the geometrical properties and parameters of the helical-fiber/matrix system are given the same values as those in Fig.4. The force-displacement curves exhibit similar three-domain behavior to those in Fig.4. However, the values of pull-out forces at which the fiber/matrix interface begins debonding, fully debonding and frictional sliding are much lower. Furthermore, the frictional sliding behaviors seem less sensitive to the value of the MFA of helical fiber than those exhibited by the curves in Fig.4. This is because the boundary condition of free twisting at the loading end leads to a considerable release of the twist strain of the fiber. The energy dissipation curves of the fiber/matrix system during fiber pull-out in the cases of two boundary conditions at the loading end are also plotted in Fig.12. The value of MFA is taken as $30°$. The plots show that a fixed boundary condition at the loading end can induce much greater energy dissipation than that resulting from the free boundary condition. This finding indicates that the twisting deformation of the fiber plays an important role in the high toughness of wood and bone.

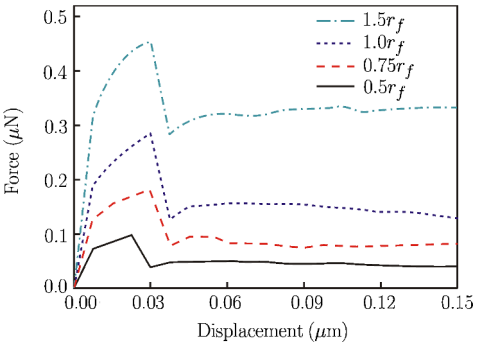

Fig. 10. Pull-out force-displacement curves for different fiber cross-section radii and the same fiber length.

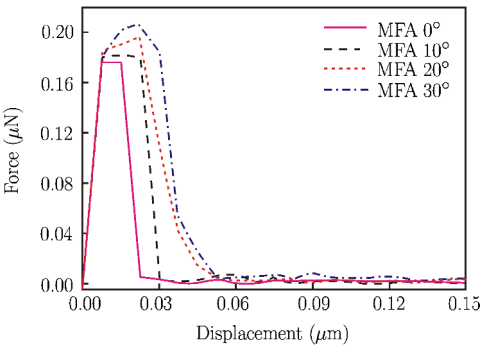

Fig. 11. Pull-out force-displacement curves for different MFAs when twisting of the loading end is not constrained.

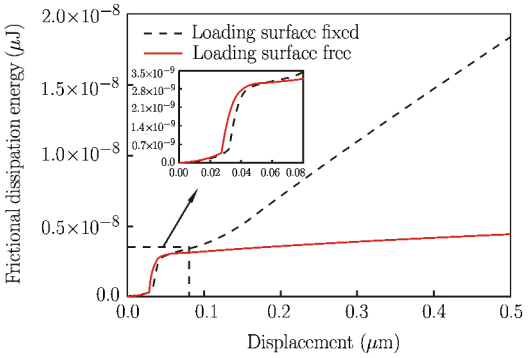

Fig. 12. Comparison of energy dissipation during pull-out of helical fiber for different boundary conditions of the fiber end at which the loading is applied.

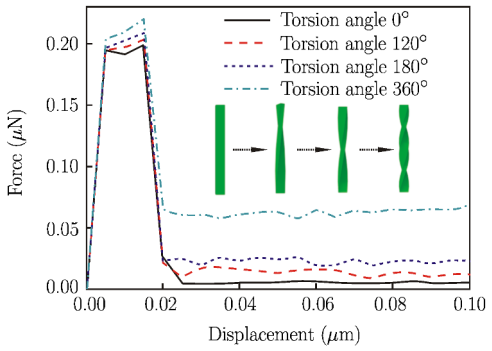

Fig. 13. Force-displacement curves for the pull-out of twisted fiber.

To further illustrate the effects of the twisting deformation of fiber, we consider a simple case in which the embedded fiber takes the shape of twisted belt, that is, the center line of fiber has only torsion and no curvature. With material properties and boundary conditions of the fiber/matrix system the same as those in Fig.4, the force-displacement curves of pull-out of twisted fiber are plotted in Fig.13 for different torsion angles per unit length. The figure shows that pure twisting deformation of the fiber can indeed distinctly enhance the pull-out force, a situation that corresponds to the bridging force during the fracture process of composites such as wood and bone. In particular, during the frictional sliding stage, the pull-out force of the fiber increases to a large value, resulting in considerable energy dissipation.

As the main origin of energy dissipation, the frictional sliding between helical fiber and matrix has significant effects on the high toughness of wood and bone. Coarse-grained atomic simulation shows that slip-stick behavior between cellulose and hemicellulose may exist when the hydrogen bonding is broken by the shear stain at a critical value[13]. We plot the force-displacement curves during fiber pull-out with different velocities in Fig.14. During the computation, MFA = 30°. In Fig.14, when the fiber end is loaded at a velocity of 0.1 μm/s, the pull-out force maintains an almost smooth variation with the displacement. However, when the loading velocity reaches a critical value of 0.2 μm/s, the zigzag slip-stick behavior between helical fiber and matrix occurs. For a loading velocity with a high value of 0.3 μm/s, the slip-stick behavior becomes more prominent. During the simulation of fiber pull-out, we here ignore microscopic effects such as atomic forces. Thus, the slip-stick behavior mainly derives from the inhomogeneous distribution of shear strain of the fiber induced by the loading velocity, i.e., the rate effect.

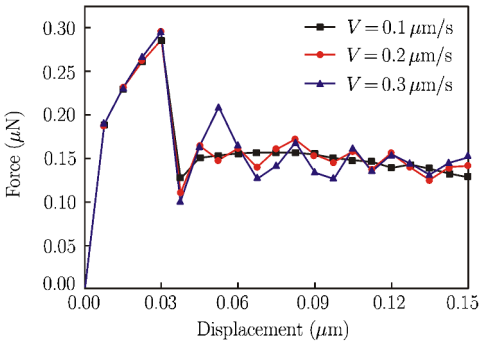

Fig. 14. Effect of loading velocity on the stick-slip behavior between fiber and matrix.

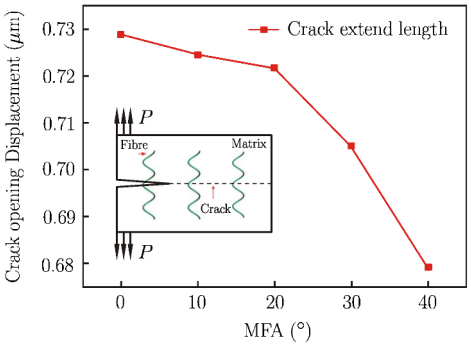

Fig. 15. Variation of crack growth length with helical angle of fiber.

Finally, we coarsely examine the effects of a helical fiber on crack propagation in a simple composite system, in which three helical fibers are embedded in the matrix. A composite system with both length and width much greater than thickness is considered, as shown in Fig.15. Furthermore, the thickness of the composite is also much greater than the characteristic length of the fiber helix. Assuming that the composite undergoes plane strain deformation, the pre-existing crack in the matrix propagates along the center line of the composite under the action of tension loading in reverse directions. The material properties of fiber and matrix are the same as those in Fig.4. The variation of crack propagation length with the value of MFA of the helical fiber is plotted in Fig.15, which shows that with an increase in the helical angle of the fiber, the crack propagation length distinctly decreases, indicating the enhanced toughening effects of the helical fiber. As shown in Figs.5 and 7, a fiber/matrix system with large helical angle or MFA can absorb quite high energy, and thus hinder crack growth, leading to a prominent toughening effect. In wood, an array of helical cellulose microfibrils rather than a single one is located in each cell wall. The accumulation of the toughening effects of so many cellulose microfibrils can certainly help their composite to achieve considerably high toughness. It should be mentioned that the failure of wood is usually involved in multi-level processes. The constitutive relationship of the cohesive law of the helical-fiber/matrix interface derives from the interaction between the cellulose and hemicellulose at molecular level. To gain a deeper insight into the quantitative influence of the micro- and nanostructures on the deformation and fracture, a multi-level failure analysis similar to that of carbon nanotube composites[27] warrants further research efforts. The toughening mechanism of helicoid microstructures can be extended to other biological materials with hierarchical chiral structures, such as climbing tendrils and tendons, to explain how the hierarchically helical microstructures contribute to the high toughness of materials. It can be expected that such toughening mechanisms will lead to the development of bio-inspired hierarchically structured chiral materials with enhanced properties, in a sequence similar to that seen for carbon-nanotube-based macroscopic materials with hierarchical structures[37–39]. That work must be left to the near future.

IV. Conclusion

We conducted the FEM simulation of the pull-out of helical fiber from a cylinder matrix. It was found that, by virtue of the uniform curvature and torsion, the helical shape of the fiber can lead not only to a relatively high pull-out force but also to a large interface area, which together contribute to the high energy dissipation during fiber pull-out. The MFA of the fiber has significant effects on the debonding and frictional sliding of the fiber and on energy dissipation. Our analyses of the pull-out of the helical fiber revealed unique insights into the effects of helical microstructures on the energy dissipation of biological materials, which explain why the widely occurring microscopic helicoid structures distinctly enhance the toughness of biological materials such as wood and bone. This work is helpful not only for our understanding of why so many biological microstructures adopt the helical shape during their assembly, but also as a benefit in providing biological inspiration for the design and fabrication of advanced composites with high toughness.

References

[1] Meyers,M.A., Chen,P.Y., Lin,A.Y.M. and Seki,Y., Biological materials: structure and mechanical properties. *Progress in Materials Science*, 2008, 53: 1-206.

[2] Chen,Q. and Pugno,N.M., Bio-mimetic mechanisms of natural hierarchical materials: A review. *Journal of the mechanical behavior of biomedical materials*, 2013, 19: 3-33.

[3] Ji,B. and Gao,H., Mechanical principles of biological nanocomposites. *Annual Review of Materials Research*, 2010, 40: 77-100.

[4] Shao,Y., Zhao,H.P., Feng,X.Q. and Gao,H., Discontinuous crack-bridging model for fracture toughness analysis of nacre. *Journal of the Mechanics and Physics of Solids*, 2012, 60: 1400-1419.

[5] Qin,Q.H. and Ye,J.Q., Thermoelectroelastic solutions for internal bone remodeling under axial and transverse loads. *International Journal of Solids and Structures*, 2004, 41: 2447-60.

[6] Song,F., Zhou,J., Xu,X., Xu,Y. and Bai,Y., Effect of a negative Poisson ratio in the tension of ceramics. *Physical review letters*, 2008, 100: 245502.

[7] Wang,J.S., Wang,G., Feng,X.Q., Kitamura,T., Kang,Y.L. and Yu,S.W., Hierarchical chirality transfer in the growth of Towel Gourd tendrils. Scientific Reports, 2013, 3.

[8] Fratzl,P., Biomimetic materials research: what can we really learn from nature's structural materials? *Journal of the Royal Society Interface*, 2007, 4: 637-42.
[9] Sanchez,C., Arribart,H. and Guille,M.M.G., Biomimetism and bioinspiration as tools for the design of innovative materials and systems. *Nature materials*, 2005, 4: 277-88.
[10] Zheng,Q.S., Yu,Y. and Feng,X.Q., The role of adaptive-deformation of water strider leg in its walking on water. *Journal of Adhesion Science and Technology*, 2009, 23: 493-501.
[11] Kong,X., Liu,J., Zhang,W. and Qu,Y., Load-bearing ability of the mosquito tarsus on water surfaces arising from its flexibility. *AIP Advances*, 2015 ,5: 037101.
[12] Neville,A.C., Biology of Fibrous Composites: Development beyond the Cell Membrane. Cambridge University Press, 1993.
[13] Adler,D.C. and Buehler,M.J., Mesoscale mechanics of wood cell walls under axial strain. *Soft Matter*, 2013, 9: 7138-7144.
[14] Galloway.,J., Helical imperative: paradigm of growth, form and function. *eLS*, 2010: 1-11.
[15] Grason,G.M., Braided bundles and compact coils: The structure and thermodynamics of hexagonally packed chiral filament assemblies. *Physical Review E*, 2009, 79: 041919.
[16] Li,L., Weaver,J.C. and Ortiz,C., Hierarchical structural design for fracture resistance in the shell of the pteropod Clio pyramidata. *Nature communications*, 2015, 6: 6216.
[17] Turner,M.D., Saba,M., Zhang,Q., Cumming,B.P., Schröder-Turk,G.E. and Gu,M., Miniature chiral beamsplitter based on gyroid photonic crystals. *Nature Photonics*, 2013, 7: 801-805.
[18] Lakes,R.S. and Benedict,R.L., Noncentrosymmetry in micropolar elasticity. *International Journal of Engineering Science*, 1982, 20: 1161-1167.
[19] Sharma,P., Size-dependent elastic fields of embedded inclusions in isotropic chiral solids. *International Journal of Solids and structures*, 2004, 41: 6317-6333.
[20] Slepyan,L., Krylov,V and Parnes,R., Helical inclusion in an elastic matrix. *Journal of the Mechanics and Physics of Solids*, 2000, 48: 827-865.
[21] Kagawa,Y., Nakata,E. and Yoshida,S., Fracture behavior and toughness of helical fiber reinforced composite metals. In: Progress in Science and Engineering of Composites. ICCM-IV, Tokyo, 1982: 1457-1464.
[22] Ball,P., Materials of the Future. In: UNESCO Encyclopedia of Life Support Systems, 2001.
[23] Fu,S.Y., Zhou,B.L. and Lung,C.W., On the pull-out of fibres with branched structure and the interface of strength and fracture toughness of composite. *Composites Science and Technology*, 1993, 47: 245-250.
[24] Fu,S.Y. and Lauke,B., The fibre pull-out energy of misaligned short fibre reinforced polymers. *Journal of Materials Science*, 1997, 32: 1985-1993.
[25] Xu,B.W., Ju,J.W. and Shi,H.S., Progressive micromechanical modeling for pullout energy of hooked-end steel fiber in cement-based composites. *Internal Journal of Damage and Mechanics*, 2011, 20: 922-938.
[26] Chen,X.Y., Beyerlein,J.I. and Brinson,L.C., Curved-fiber pull-out model for nanocomposites. Part 2: Interface debonding and sliding. *Mechanics of Materials*, 2009, 41: 293-307.
[27] Chen,Y.L., Liu,B., He,X.Q., Hung,Y. and Hwang,K.C., Failure analysis and the optimal toughness design of carbon nanotube-reinforced composites. *Composites Science and Technology*, 2010, 70: 1360-1367.
[28] Yang,Q.S., Qin,Q.H. and Peng,X.R., Size effects in the fiber pullout test. *Composite Structures*, 2003, 61: 193-198.
[29] Shi,D.L., Feng,X.Q., Huang,Y., Huang,K.C. and Gao,H.J., The effect of nanotube waviness and agglomeration on the elastic property of carbon nanotube-reinforced composites. *Journal of Engineering Materials and Technology*, 2004, 126: 250-257.
[30] Goh,K.L., Aspden,R.M. and Hukins,D.W.L., Review: finite element analysis of sterss transfer in short-fibre composite materials. *Composites Science and Technology*, 2004, 64: 1091-1100.
[31] Marklund,E. and Varna,J., Modeling the effect of helical fiber structure on wood fiber composite elastic properties. *Applied Composite Materials*, 2009, 16: 245-262.
[32] ABAQUS, Hibbitt Karlsson Sorenson, Inc., 1997.
[33] Stefanie,E., Microstructure and fracture mechanical response of wood. *International Journal of Fracture*, 2006, 139: 495-508.
[34] Reiterer,A., Lichtenegger,H., Tschegg,S. and Fratzl,P., Experimental evidence for a mechanical function of the cellulose microfibril angle in wood cell walls. *Philosophical Magazine A*, 1999, 79: 2173-2184.
[35] Wang,Z., Gu,L.L., Gao,Z.Z., Liu,B. and Wang,Y.L., Experimental study on Poisson's ratio of lumber by dynamic testing. *Chinese Journal of Scientia Silvae Sinicae*, 2015, 51: 102-107.
[36] Maritan,A., Micheletti,C., Trovato,A. and Banavar,J.R., Optimal shapes of compact strings. *Nature*, 2000, 406: 287-290.
[37] Li,Q., Kang,Y.L., Qiu,W., Deng,W.L. and Zhong,X.H., Deformation mechanisms of carbon nanotube fibers under tensile loading by insitu Raman spectroscopy analysis. *Nanotechnology*, 2011, 22: 225704.

[38] Qiu,W., Li,Q., Lei,Z.K., Deng,W.L. and Kang,Y.L., The use of a carbon nanotube sensor for measuring strain by micro-Raman spectrosopy. *Carbon*, 2013, 53: 161-168.

[39] Deng,W.L., Qiu,W., Li,Q., Li,Y.L. and Han,S.S., Multi-scale experiments and interfacial mechanical modeling of carbon nanotube fiber. *Experimental Mechanics*, 2014, 54: 3-10.